Field-dependent domain structure evolution in artificial ferrimagnets analyzed by spin-polarized tunnel transport in magnetic tunnel junctions

C. Tiusan, T. Dimopoulos, K. Ounadjela, Michel Hehn

Field-dependent domain structure evolution in artificial ferrimagnets analyzed by spin-polarized tunnel transport in magnetic tunnel junctions

C. Tiusan, T. Dimopoulos, and K. Ounadjela
Institut de Physique et Chimie des Materiaux de Strasbourg, 23 rue du Loess, F-67037, Strasbourg Cedex, France

M. Hehn
Laboratoire de Physique des Matériaux, CNRS (UMR 7556), Université H. Poincaré, F-54506 Nancy, France
(Received 5 July 2000; revised manuscript received 6 February 2001; published 23 August 2001)

A powerful technique for investigating field-dependent micromagnetism in thin magnetic layers is presented. The technique uses the spin-polarized tunnel-transport mechanism in magnetic-tunnel junctions. We used this technique to study the micromagnetic-reversal mechanism in an artificial ferrimagnetic system, which consists of two ferromagnetic layers strongly antiferromagnetically coupled through a nonmagnetic interlayer. We show that the high sensitivity of the spin-polarized current to the fluctuations of magnetization allows to probe the magnetic-domain structure in the magnetic electrodes. As a contrast to standard *M-H* and giant-magnetoresistance measurements, which are only able to probe the global magnetic state of this artificial ferrimagnet, we show here that the tunnel magnetoresistance discriminates the field-dependent evolution of the domain phases in selective magnetic layers. Furthermore, we demonstrate the capability of a tunnel-magnetoresistance signal to be used as a quantitative probe for investigating residual walls during the reversal process.

DOI: 10.1103/PhysRevB.64.104423 PACS number(s): 75.60.−d, 73.40.Gk, 73.40.Rw, 77.80.Dj

I. INTRODUCTION

Extensive experimental work has been done on magnetotransport properties of magnetic tunnel junctions (MTJ) since the discovery of the large tunnel magnetoresistance (TMR) at room temperature.[1,2] Up to now, studies were especially focused on transport properties, such as bias voltage and temperature dependence of tunnel resistance and magnetoresistance. Recently, magnetism in ferromagnetic electrodes has defined a new exciting research area in this field.[3–9] The key factor is that the spin-polarized tunneling is sensitive to the local magnetic configuration of each magnetic layer in contact with the tunnel barrier.[6] Extreme resistive states of the MTJ are then observed for ferromagnetic and antiferromagnetic alignment of the magnetizations of the electrodes. However, intermediate situations may exist for which the magnetic layers include domain-wall structures. The correlation between domain-structure and magnetic-field-dependent-transport properties can be done taking into account different tunneling paths associated with local magnetization configurations.[6] According to this model, domains and domain walls give rise to tunneling channels with different resistances determined by the lateral fluctuations of the angle between the magnetic moment of the magnetic layers in contact with the tunnel barrier.

The technique described in this work uses an MTJ as a powerful *tool* to investigate micromagnetic properties of a magnetic thin film. The design of that device has an optical analog: the *polarizer-analyzer* system. The investigated magnetic layer is used as a hard layer in the MTJ and it acts as a *spin polarizer*. It is separated by an insulating barrier from a magnetically soft subsystem, having a small coercive field and a sharp magnetization reversal. When this soft layer is in a single-domain state, it acts as a *spin analyzer* (detection layer) for electrons injected across the barrier from the hard subsystem (spin polarizer). Then, all features that appear in the field-dependent resistance of the MTJ are due to domain walls or fluctuations in domain magnetization located in the hard magnetic layer, *interfaced* with the tunnel barrier. The strength of this technique is to selectively analyze the magnetism of layers in contact with the tunnel barrier in contrast with imaging techniques that integrate the signal over several layers.

In this paper, we have investigated the magnetic-domain-structure evolution in an artificial ferrimagnet (AF) trilayer. This system[6,10,11] is constituted by two ferromagnetic metals, having unequal magnetic moments antiferromagnetically coupled across a nonmagnetic spacer. They are widely used nowadays as magnetically hard electrodes in MTJ and spin-valve devices due to their high thermal stability and magnetic rigidity.[10,12] Their small net magnetic moment reduces the parasitic coupling with the soft layer, which in general could be detrimental in MTJ and giant-magnetoresistance (GMR) sensor capabilities. Typical GMR measurements performed in spin-valve systems or multilayers using artificial antiferromagnetic systems[13] are only able to probe the global domain structure of the entire device without being able to discriminate the individual magnetic-field evolution of domain phases in each magnetic layer of the hard subsystem. In contrast, by building a magnetic-tunnel junction based on an AF, having either the thicker or the thinner magnetic layer in contact with the tunnel barrier, we show here that the magnetic behavior of each layer can be extracted selectively. This is performed by analyzing the magnetoresistive signal shape and amplitude corresponding to each stacking sequence of the AF. Furthermore, quantitative information on the evolution of the domain-wall density with the external field has been extracted from the TMR signal in agreement with values obtained from magnetic-force-microscopy (MFM) mea-

surements, performed in the operational field window of the MTJ device.[6]

This paper is organized as follows. Section II describes the stack design and sample preparation as well as measurement conditions. Section III provides the analytical description of the field-dependent magnetic behavior of an artificial ferrimagnet without introducing any domain structure. Then analysis of data involving experimental magnetization curves and current in-plane GMR on the AF are compared to the analytical description to illustrate the presence of domain walls. How selective is the current-perpendicular to plane-tunnel MR measured on the MTJ stack is described in Sec. IV together with a clear analysis of the field-dependent magnetic features of the hard subsystem in the entire field window.

II. SAMPLE PREPARATION, MEASUREMENTS

Tunneling junctions are constituted from complex stacks defined as follows. First, a Cr(1.6 nm)/Fe(6 nm)/Cu(30 nm) buffer layer is grown on a previously sputter-etched 3 in. diameter Si(111) wafer.[10] On the top of the buffer, the AF trilayer Co(1.8 nm)/Ru(0.8 nm)/Co(3 nm) (denoted by *N*-AF) or the ''reversed'' configuration Co(3 nm)/Ru(0.8 nm)/Co(1.8 nm) (denoted *R*-AF) is stacked. The Al-oxide barrier was formed by a rf Ar/O_2 plasma oxidation of a previously sputtered Al metallic layer.[10,15] A magnetically soft bilayer [the so-called detection layer (DL)] is sputtered on top of the Al-oxide tunnel barrier and consists of Co(1 nm)/Fe(6 nm). Finally, the multilayer stack is capped for protection with Cu(5 nm)/Cr(3 nm).

Magnetic properties of as-deposited multilayer films were studied at both macroscopic and microscopic scales. Macroscopic magnetization curves were measured using an alternating gradient-field magnetometer at room temperature. At a microscopic scale, the domain structure has been observed by MFM, in a tapping-lift phase-detection mode, in zero and in-plane applied fields up to $|H|=800$ Oe, available in our experimental setup.

As-deposited 3-in. wafers, containing the stack described above, were patterned by UV lithography into arrays of squared junctions with tunnel-barrier surface areas of $10\times10\ \mu m^2$. The junctions, measured using a conventional four-point technique, present a large (25–30 %) tunnel magnetoresistance at room temperature.

III. ANALYTICAL RESPONSE OF TUNNEL JUNCTIONS USING ARTIFICIAL FERRIMAGNETS

How an artificial ferrimagnet system behaves when submitted to a magnetic field can be simply calculated under the assumption that the magnetization reversal in the magnetic layers occurs via a coherent-rotation mechanism. Because of the strong torque created by the antiferromagnetic coupling on the magnetization of the two coupled layers, a coherent rotation of the magnetization should be favored with respect to a mechanism based on nucleation and propagation of walls in the antiferromagnetically coupled subsystem. This type of magnetization reversal can be calculated using the

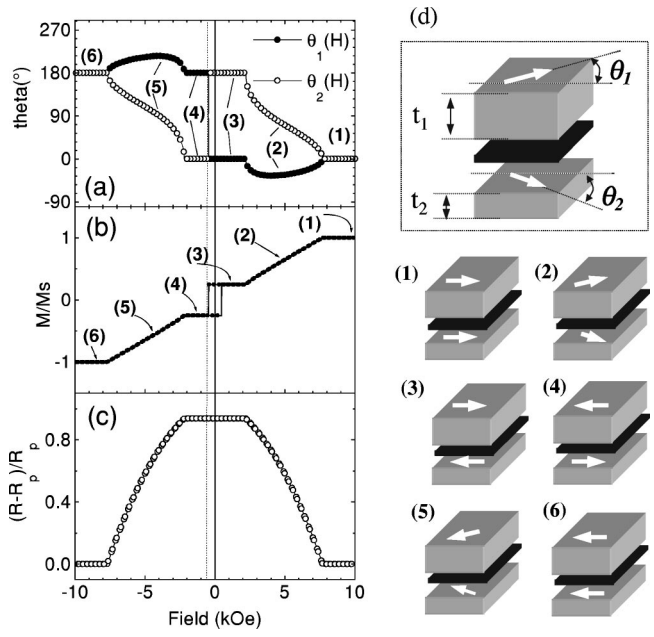

FIG. 1. Theoretical calculation of field-dependent magnetic behavior of an AF system, by using the Stoner-Wolfarth model (Ref. 18). (a) Variation of angle between the magnetizations of the ferromagnetic layers constituting the AF hard subsystem and the external applied field direction. (b) Magnetization versus field (M-H) curve using the expression $M(H)=M_s[t_1\cos\theta_1(H)+t_2\cos\theta_2(H)]/(t_1+t_2)$. (c) Theoretical magnetoresistive response (GMR) of the AF using an expression of the type $(1-\cos[M(H)/M_s]^2)$. The sketch in the right-hand side of the (d) shows the ideal micromagnetic configuration of the AF at critical field values [states (1)–(6)].

energy functional, reported in Eq. (1), of an antiferromagnetically coupled trilayer with in-plane magnetization submitted to an external field H,[16,17]

$$\varepsilon(H)=J\cos[\theta_1-\theta_2]-M_sH[t_1\cos\theta_1+t_2\cos\theta_2]+K_1t_1\sin^2\theta_1+K_2t_2\sin^2\theta_2, \quad (1)$$

where θ_1, θ_2 describe the orientation of the magnetization relative to the field direction in each layer of thickness t_1 and t_2, respectively. The first two terms contain the interlayer coupling energy and the Zeeman energy in an applied field H. The second two terms describe the in-plane uniaxial anisotropy energies of the two magnetic layers. The values taken for the modeling have been set close to the measured experimental data extracted from the magnetization curves ($t_1=3$ nm, $t_2=1.8$ nm, $J=-1.1$ erg/cm^2, $K_1=K_2=10^5$ erg/cm^3, $M_s=1430$ emu/cm^3).

The magnetization-angle variation as a function of field, $\theta_1(H)$, $\theta_2(H)$ shown in Fig. 1(a), can be calculated by minimizing numerically the energy functional. Figures 1(b) and 1(c) show field-dependent magnetization $M(H)$ and magnetoresistance $R(H)$ curves, respectively, deduced from the angle variation.

Let us consider the $\theta(H)$, M-H, and R-H curves counterclockwise from the positive high-field saturation, where all magnetic moments are parallel and oriented in the positive field direction [Fig. 1, state (1)].

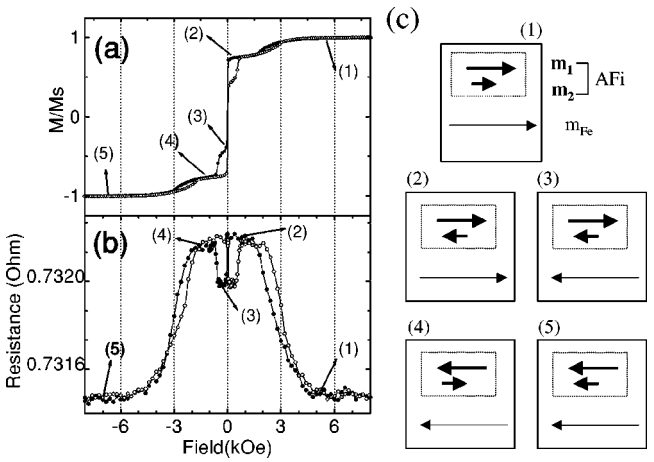

FIG. 2. Experimental *M-H* (a) and magnetoresistance GMR (*R-H*) curve with the current-in-plane (b) for the Si/Cr/Fe/Cu/Co/Ru/Co stack. In the figures the branch measured from positive to negative field is (–●–) while the branch measured from negative to positive field is (–○–). The sketch in the right-hand side of the (c) shows the micromagnetic configuration of the states (1)–(5) as predicted by the theoretical calculations. Hysteresis effects in the flank of both MR and *M-H* curves, not present in the theoretical curves, are related with domain structure developed in the AF layers during the magnetization reversal in the saturation-plateau [states (1)–(2)] region.

By decreasing the applied field in the flank region of the *M-H* curve [field window between (1) and (3)], the angle of the thinner layer of the AF varies continuously from 0 to π with respect to the positive high-field saturation direction. At the same time, the moment of the thicker layer starts to rotate up to a maximum deflection angle, then it is dragged back to its initial state by the strong AF coupling. This field region corresponds to a transition from a parallel configuration (saturated state) to an antiparallel configuration [plateau shown in Fig. 1, state (3)] of the magnetizations of the two layers strongly antiferromagnetically coupled. As expected from the angle dependence of the magnetizations in the two layers, it is shown from the *M-H* and *R-H* curves that the net moment decreases from the parallel state (1) to the antiparallel state (2) while the resistance increases. The width of the plateau depends on the strength of the antiferromagnetic (AFM) coupling with respect to the Zeeman energy. In this region, the AF behaves like a magnetic rigid body of reduced moment (m_1-m_2) and switches in a reversed magnetic field, which depends on the intrinsic properties of the material and the strength of the AFM coupling.[11] The reversal of the AF is shown in Figs. 1(a) and 1(b) for which an abrupt 180° change occurs for the angles of both layers [transition from state (3) to state (4)]. However, the MR curve [Fig. 1(c)] indicates no change in the resistance at the coercive field since the relative angle remains unchanged.

These results, showing features corresponding to pure rotation of magnetization, are compared with experimental data extracted from *M-H* [Fig. 2(a)] and magnetoresistance (GMR) [Fig. 2(b)] measurements. In this case, measurements are performed on a continuous Cr/Fe/Cu/Co(1.8 nm)/Ru(0.8 nm)/Co(3 nm)/Al multilayer stack with the current in plane using a conventional four-point technique. The experimental data show general features similar to those predicted by the theoretical curves, which indicate that the reversal mechanism follows mainly a rotational process. Indeed, from positive saturation down to an AFM plateau, the gradual decrease of magnetization in the *M-H* curve and the related increase of resistance in the *R-H* curve both indicate the variation of the relative angle of magnetizations of the two layers of the AF. The magnetic contribution of the 6-nm Fe buffer layer separated from the AF by the 30-nm-thick Cu layer is shown as a sharp reversal at low field (20 Oe). Interestingly, the presence of the Fe seed layer gives rise to an additional small MR contribution (0.02%), shown by a decrease of the resistance when the Fe magnetization switches [transition from state (2) to state (3), Fig. 2(b)] and an increase of resistance when the net moment of the AF reverses [transition from state (3) to state (4), Fig. 2(b)]. In this way, the Fe seed layer is used to probe the AF net-moment behavior at low field.

However, this simplified energy functional does not take into account aspects related to random distribution of anisotropy,[14] which is a key factor for the formation of domain-wall structures. In the flank region (1),(2) and (4),(5), irreversible processes give rise to hysteretic behavior illustrated in both GMR and *M-H* curves [Figs. 2(a) and 2(b)] and are attributed to a domain phase transformation in the AF magnetic layers. Indeed, for the same applied field, the magnetization configuration is strongly affected by the magnetic history of the AF. A reasonable assumption is to attribute the existence of the phase transformation in the AF thinner layer, since this layer reverses by 180° according to the theoretical prediction [Fig. 1(a)]. However, several questions remain unanswered. Will this domain phase transformation be duplicated in the thicker layer by the AFM coupling? How stable are the magnetic walls in each of the layers and in which field regions are they created and annihilated? The GMR and *M-H* measurements provide evidence of a domain phase transformation without being able to discriminate which layer of the AF is involved. In the next section, we will show that using tunnel-transport and MFM experiments, we are able to selectively analyze the field-dependent evolution of the domain-wall structure in each layer of the AF subsystem.

IV. TUNNEL TRANSPORT AS A PROBE FOR INVESTIGATING FIELD-DEPENDENT DOMAIN STRUCTURES

As already mentioned, the magnetic-tunnel junctions consist of an artificial ferrimagnet as a hard subsystem (Co/Ru/Co) separated by an Al-Oxide layer from a Co/Fe soft subsystem. The soft DL presents a square magnetization loop, with a coercive field of about 20 Oe and a magnetization reversal in a field range smaller than 2 Oe.[10] Therefore, for applied fields above 30 Oe, the DL can be considered as being in a single-domain state. It will act as a spin analyzer for electrons injected from the hard magnetic subsystem (spin polarizer) across the tunnel barrier. Two stacking sequences will be discussed in this paper: (i) The thicker layer of the AF interfaced with the tunnel barrier (*N*-AF), which will determine the direction of the net moment in the opera-

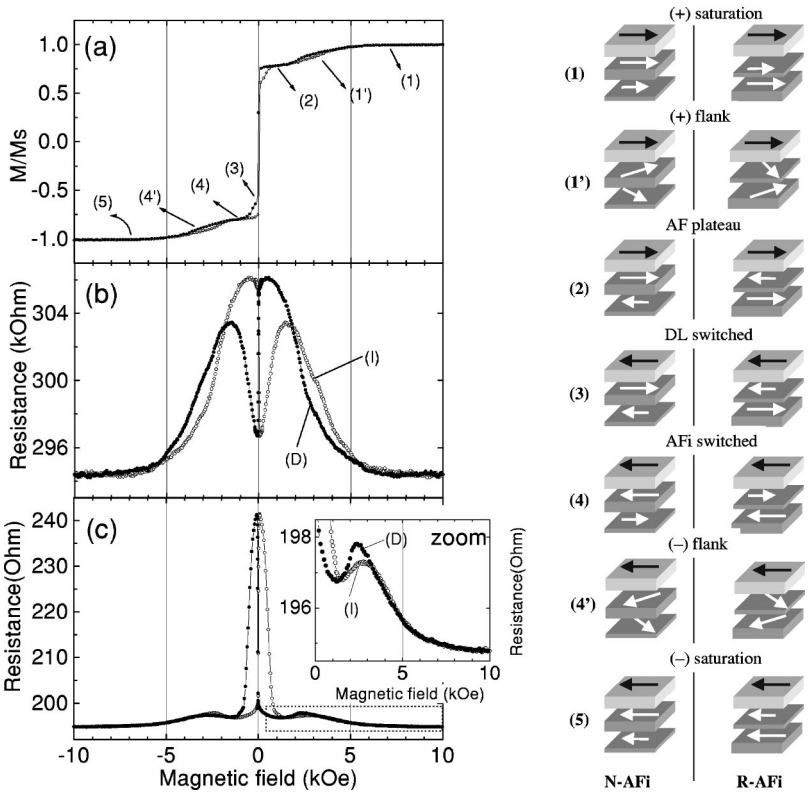

FIG. 3. Magnetization versus field *M-H* (a) and *R-H* curves (b,c) for a magnetic-tunnel junction using an AF hard subsystem. The *R-H* curves are taken in the current-perpendicular-to-plane (CPP) geometry being then only sensitive to the tunnel current. (b) and (c) are the TMR curves for the junctions with the thin and thick magnetic layers of the AF in contact with the tunnel barrier, respectively. The inset of (c) shows a zoom in the low resistive state. The sketch in the right-hand side of the figure shows the ideal micromagnetic configuration of the MTJ at critical field values [states (1)–(5)].

tional field window, (ii) the thinner layer of the AF interfaced with the tunnel barrier (*R*-AF), in which magnetization will be opposite to the direction of the net moment.

Tunnel-magnetoresistance curves were measured on MTJ's with AF having either the thin [Fig. 3(b)] or the thick Co layer [Fig. 3(c)] in contact with the tunnel barrier. This allows to selectively analyze their domain structure. As expected, there are no significant differences in the *M-H* loops [Fig. 3(a)] for the *N*-AF and *R*-AF because of the averaging signal over the entire stack. However, the *R-H* loops are completely different for the two stacking sequences, reflecting different field-dependent domain-phase evolutions in the thick and the thin magnetic layer of the AF.

A. Selective analysis of micromagnetic features at high field (flank region) in the artificial ferrimagnet

Let us first consider the *M-H* and *R-H* curves counterclockwise from the positive high-field saturation, where all the magnetic moments are parallel and oriented in the positive field direction [Fig. 3, state (1)]. The resistance of the MTJ based either on an *N*-AF or on an *R*-AF is the lowest, and corresponds to electrons that tunnel across the insulator between two ferromagnets in a parallel configuration (all magnetic moments are aligned).

By decreasing the applied field in the flank region of the *M-H* curve [field window between states (1) and (2)], a continuous gradual increase of the MTJ resistance is observed when the thinner Co layer is in contact with the barrier [*R*-AF, Fig. 3(b)]. However, for the *N*-AF junction, a small increase of resistance followed by a decrease towards the end of the flank can be observed [Fig. 3(c)]. This is in agreement with the expected variation of magnetization angles shown in Fig. 1(a) and confirms that only the thinner layer has the large magnetization rotation. As a result, in the positive part of the AFM plateau [Fig. 3, state (2)], the thicker AF layer has its magnetization aligned along the field direction (parallel with the DL) while the thinner AF layer is oriented opposite. This corresponds, in the *R-H* curves, to a low resistance state in the case of the *N*-AF [Fig. 3(c)] and to a high resistance state in the case of *R*-AF [Fig. 3(b)] after completion of the reversal occurring at field. A first evidence of the formation of domain structure in the thinner layer of the AF is shown in Fig. 3(b). In the flank region (3–5 kOe field window), the *R-H* curve of the *R*-AF, which probes the thinner magnetic layer, is hysteretic [Fig. 3(b)]. Starting from positive saturation and decreasing the field, the magnetization of the thinner layer of the AF experiences a 180° rotation giving rise to 360° Néel domain walls. These walls originate at regions where the local anisotropy coincides with the direction of the saturation field and they will constitute the core of the future walls, when adjacent regions relax their magnetization by rotating in antiphase. Indeed, when the field is reduced, these regions will rotate clockwise and anticlockwise, while the magnetization in the core region will remain blocked,[18] aligned with the direction of the field and the detection layer. In terms of tunnel resistance, in branch (*D*) these regions constitute local channels of low tunnel resistance compared to adjacent regions that have their moments misaligned with respect to the detection layer. These low-resistance channels are reflected in the *R-H* curve in Fig. 3(b): for a given applied field between 3 and 5 kOe, a significant change of the resistance is observed when comparing branch (*D*), measured when decreasing the field from

positive saturation, with branch (*I*), measured when increasing the field towards positive saturation. Indeed, when measuring branch (*I*), the initial state of magnetization of the thin layer is antiparallel to the field direction. In this case, the nucleated walls would have their center antiparallel to the detection layer and act as high-resistance state. So, the overall resistance is now higher induced by the contribution of the additional resistance of the blocked regions.

B. Duplication of domain walls in the artificial ferrimagnet: Lower-field region, end of the flank—AF plateau

How the presence of 360° walls in the thin AF layer affects the thicker layer is shown in the inset of Fig. 3(c). From the absence of hysteresis at high fields in the flank when the thicker AF layer is interfaced with the tunnel barrier (3.5 to 5 kOe), no domain structure is built in the thick layer in this field region. This is related to a limited rotation of the magnetization with respect to the field direction [limited to 45° as shown in Fig. 1(a)]. In contrast, below 3.5 kOe, the competition between the AFM coupling, local anisotropy, and Zeeman energies allows the walls to be duplicated from the thinner to the thicker layer. Duplication of the walls from the thin layer can take place due to the strong AFM coupling that tends to locally flip the magnetic moments to overcome the frustration sensed by the walls in the thin layer. These walls have their center parallel with both the external field and the magnetization of the thicker layer of the AF. This makes them energetically favored by the external field but the AFM exchange coupling tends to annihilate them when reducing the field. An estimation of the AFM exchange field ($H_{ex} = 3-4$ kOe) indicates that this duplication should take place at a field in the range of 3 kOe. Above this field range, the Zeeman energy prevents the walls from being duplicated in the thicker layer. These walls act as high-resistance channels and are reflected in the inset of Fig. 3(c) as high-resistance states compared to the reversed branch of the loop where no domain walls subsist at the end of the plateau (see next section).

At the end of the flank, the angle of the walls in the AF layers will be large enough to make their existence energetically unfavorable (the wall energy increases with the angle of the adjacent domains). Therefore, the walls are annihilated, corresponding to the closure of the hysteresis in Figs. 3(b) and 3(c). Magnetization features in the AF layers in the AFM plateau are reflected in the TMR loops for the *R*-AF-based [Fig. 3(b)] and *N*-AF-based [Fig. 3(c)] MTJ's. Indeed, fluctuations of magnetization angle in the thicker AF layer, due to local anisotropies, determine a resistive state in the plateau higher than in the saturation state (perfect parallel alignment) as shown in the inset of Fig. 3(c). Moreover, a gradual increase of the junction's resistance, when reducing the field towards zero, is determined by the relaxation of magnetic moments in both AF layers towards their local anisotropy axes [see Figs. 3(b) and 3(c)].

C. Negative low-field-reversal domain structures and the flank towards negative saturation

By reversing the magnetic field in the negative direction, the magnetically soft DL reverses its magnetization [Fig. 3, transition from state (2) to state (3)]. This will induce a magnetization configuration between the magnetic layers interfaced with the tunnel barrier, antiparallel in the case of *N*-AF-based MTJ responsible for a high-resistance state [Fig. 3(c)], and a parallel magnetization configuration in the case of R-AFi-based MTJ, responsible for a low-resistance state [Fig. 3(b)]. By further increasing the negative applied magnetic field, the Zeeman energy will then overcome the coupling energy and the AF net magnetic moment reverses spontaneously by rotation of magnetizations in each layer, leading to a rapid increase (*R*-AF) or decrease (*N*-AF) of the MTJ resistance. As soon as the reversal of the net moment is completed [Fig. 3, state (4)] , the magnetization of the AF topmost layer becomes either parallel (small-resistance configuration in the case of *N*-AF-based MTJ) or antiparallel with the DL (high-resistance configuration of the *R*-AF-based MTJ).

However, since the two Co layers rotate by 180° for the reversal of the net AF moment, creation and annihilation of 360° domain walls in both thick and thin magnetic layers are expected.[6,18] Furthermore, as a consequence of the strong interlayer AFM coupling, walls nucleated in one layer are mirrored in the other. The AFM coupling has a strong impact on the walls stability. Indeed, during the reversal, the thick layer develops walls having their centers opposite to the negative field direction. This situation is energetically unstable, as the core of the wall has its magnetization direction antiparallel to the field. However, this instability is further maintained by the AFM exchange, which couples the walls in the thick and thin layers since the walls in the thin layer are energetically stable (their center is oriented along the field direction). So, the AFM coupling acts as an additional source of pinning for the walls located in the thick layer up to fields for which the Zeeman energy overcomes the AFM coupling energy.

This particular domain-phase evolution and the stability of the walls in each layer is reflected in the *R-H* curves (Fig. 3) and confirmed using field-dependent MFM with *in situ* applied field. After reversal of the DL, the cores of the 360° walls act as high-resistance tunnel channels in the *N*-AF configuration and as low-resistance tunnel channels in the *R*-AF configuration. The stability of the walls in the thin AF layer is evidenced on the TMR curve [Fig. 3(b)] by the fact that the highest-resistance state is never achieved (maximum resistance 304 kΩ as compared to 306 kΩ) after the AF reversal. In this magnetic configuration, the core of the walls is parallel to the DL acting as highly conducting channels, reducing as a consequence the resistance of the MTJ. These stable walls will gradually disappear only when, at high fields, the domains adjacent to the walls will start reversing by rotation, annihilating eventually the large-angle walls. This effect is shown on Fig. 3(b) by the slow decrease of the resistance at the negative flank towards saturation. In contrast, the walls are less stable in the thick AF layer and can vanish at lower fields in the negative AFM plateau, soon after the AF's net-moment reversal. This effect is clearly indicated in the TMR curve by reaching the low-resistance state in the negative AFM plateau, as shown in Fig. 3(c).

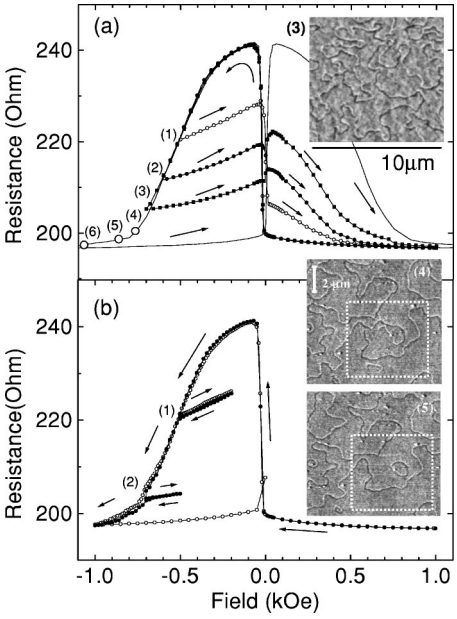

FIG. 4. (a) Minor *R-H* loops (CPP), taken in the AF plateau, for a MTJ using an AF having the thick magnetic layer in contact with the tunnel barrier (*N*-AF configuration). Asymmetric loops start for all curves at + 1 kOe and are reversed at different negative field values: −500 Oe (1), −600 Oe (2), −700 Oe (3), −800 Oe (4), −900 Oe (5), −1 kOe (6). These curves illustrate the existence of 360° walls in the thick AF layer up to fields of −1 kOe. (b) Minor *R-H* loop (CPP) taken in the AF plateau (+1/−1 kOe) starting at +1 kOe, reversed at some negative-field values during the magnetization reversal of the AF: −500 Oe (1), −700 Oe (2) decreased up to fields of −200 Oe and −500 Oe, respectively, and then increased again up to −1 kOe. This reversible phenomenon, which shows that the walls are not propagating, is aimed to emphasize the rotation mechanism of the magnetization reversal. Inset: Magnetic-force-microscopy images showing the 360° residual domain structure in state (3) and the evolution of the domain structure between two magnetic states (4) and (5). The MFM images corresponding to the states (4) and (5) illustrate the annihilation of wall segments with the applied field.

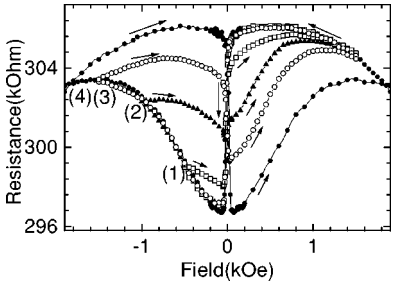

FIG. 5. Minor *R-H* loops (CPP), taken in the AF plateau, for an MTJ using an AF having the thin magnetic layer in contact with the tunnel barrier (*N*-AF configuration). Asymmetric loops are taken between +1 kOe and different negative field values, defined by the states −500 Oe (1), −1 kOe (2), −1.5 kOe (3), −2 kOe (4), during the net AF moment reversal. This figure is aimed to emphasize the stability of the walls in the thin layer of the AF. It is interesting to note that the walls are more stable in the thin layer up to fields of 2 kOe, compared with lower-field annihilation in the thick layer (Fig. 4).

D. Stability of the 360° walls using minor TMR loop features

Details of the magnetization reversal and domain-wall stability are reflected in Figs. 4 and 5 for the *N*-AF- and *R*-AF-based MTJ junctions, respectively. These figures represent measurements of minor *R-H* curves for the *N*-AF between +1 and −1 kOe (Fig. 4) and for the *R*-AF between +2 and −2 kOe (Fig. 5) after saturation in a positive field. Starting from the positive field, the MTJ is in a low(*N*-AF)- or high(*R*-AF)-resistance state depending on which of the AF's layers is in contact with the barrier. These resistance states are inverted when the DL switches at low negative field.

Before negative saturation, the field sequence is inverted at some states denoted by states (1), (2), (3), or (4) in Figs. 4 and 5. Reversing the field towards positive values, the resistive jump occurring when the DL switches at positive field depends on the degree of reversal of the AF net magnetization and therefore on the residual domain-wall structure. The jump even changes sign when a particular point has been overcome upon reversal. The amplitude and especially the sign of the jump in the *R-H* curve has a particular importance. In Fig. 4 (Fig. 5), corresponding to *N*-AF (*R*-AF)-based MTJ's, respectively, when the reversal is stopped in state (1) a steep drop (increase) of the MTJ resistance after the DL reversal in the positive field indicates that the switch of the DL has activated predominant low (high) conduction channels, associated with the network of walls, which contribute to the resistance along with the high- (low-) conduction channels provided by the domains. Interestingly, the reversed effect, an increase (drop) of the resistance when the DL switches, shown in Fig. 4 (Fig. 5) after previously stopping in state (3), is due to the activation of predominant domain conduction channels. The two contributions in the resistance from domains and walls, almost balance in the case when the reversal is stopped at state (2). This will not give rise to any jump in the resistance when the DL switches, as we can see from Figs. 4 and 5.

The stability of the walls is given through the field range needed to get a symmetric TMR curve. In the *N*-AF case, the field range between −1 and 1 kOe was sufficient to completely reverse the thicker AF layer, which indicates that most of the 360° walls have been annihilated. This is confirmed by the symmetry of the TMR curve when increasing the field towards saturation. In contrast, the experiments performed on the *R*-AF system show that the stability of the domain walls in the thinner AF layer exceeds the previous field range, where the layers were supposed to have completely reversed as shown from the asymmetric shape of the curves for fields below 2 kOe, Fig. 5 [states (1), (2), (3)]. In this states the subsistence of walls in the thinner layer is responsible for the asymmetric TMR signal of the junctions incorporating the *R*-AF. Interestingly, the asymmetry vanishes only for fields beyond 2 kOe [Fig. 5, state (4)], which indicates that the walls have been annihilated for fields larger than 2 kOe.

Quantitative analysis of the AF net magnetization reversal[17] and the domain-wall stability features has been made by using an analytical model for the MTJ in a multi-

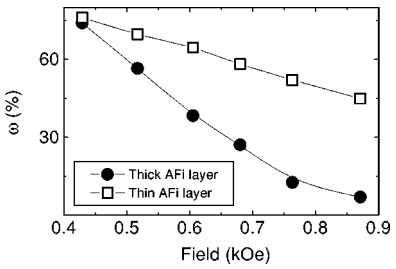

FIG. 6. Variation of the density of walls in external field in the thicker and the thinner AF magnetic layers.

domain configuration.[19] In this model, domain and domain walls constitute tunneling channels having different resistances. The domain magnetization makes an angle θ with respect to the field direction, while the magnetization in the center of the wall remains aligned along the initial positive saturation direction. Therefore, the total resistance R of the MTJ in a multidomain configuration is calculated as the equivalent resistance of a network of in-cascade resistances associated with domain and domain-wall elementary segments.

The residual domain-wall structure subsisting in the AF in a state (i) (i$=1, \ldots, 5$, Figs. 4 and 5) is reflected by a higher (for an N-AF) or a lower (for an R-AF) resistive state of the MTJ than the one corresponding to the configuration where the walls are completely annihilated (R_0). We quantify this wall-related resistive state by a residual magnetoresistance $t_R^{(i)}=[R(i)-R_0]/R_0$. Therefore, the surface of the walls with respect to the total surface of the junction $\omega^{(i)}$, responsible for a residual magnetoresistance $t_R^{(i)}$, can be deduced from the equation[19]

$$\omega^{(i)}=\frac{t_R^{(i)}-\dfrac{T_{MR}(1-\cos\theta^{(i)})}{2}}{\dfrac{T_{MR}(1+\cos\theta^{(i)})}{2}}\,\frac{1+T_{MR}}{1+t_R^{(i)}} \qquad (2)$$

where $T_{MR}=(R_{AP}-R_P)/R_P$; R_{P} and R_{AP} represent the tunnel resistance corresponding to the parallel (P) and antiparallel (AP) configuration, respectively, of the MTJ barrier-adjacent magnetic layers.

As shown by the MFM measurements, in the state (3) (inset of Fig. 4), the domain magnetization is practically reversed. So $\theta(i>3)\simeq 0$ and ω can be easily calculated for the N-AF and R-AF from Eq. (2).

The variation of ω as a function of the applied field is reported in Fig. 6. The results are in agreement with values extracted from the analysis of the MFM images (inset of Fig. 4).

The results presented in Fig. 6 are of particular importance because they illustrate the relative stability of the walls in the thick and thin layer of the AF. For relatively small negative applied fields ($|H|<0.5$ kOe), ω is high and almost similar in both layers. This result confirms the fact that in this field range the domain-wall structure is antiferromagnetically mirrored in both AF layers. However, we have to specify that the calculated values are slightly overestimated since for $H<0.5$ kOe, the angle of the magnetization in the AF layers with respect to the external field ($\theta^{(i)}$) cannot be neglected.

For higher fields ($H>0.6$ kOe), $\theta^{(i)}$ can be reasonably considered zero. In this field range, no significant change in the evolution of ω with the applied field was found when taking into account a nonzero value of $\theta^{(i)}$.

From Fig. 6 we can clearly see that the variation of the density of walls with respect to the field [$\omega(H)$] is strongly different in the thicker and the thinner AF layers. Domain walls located in the thin AF layer are more stable than those located in the thicker one. For an applied field of 0.9 kOe, the walls are completely annihilated in the thick layer while almost 45% of the thin-layer surface area is still occupied by residual walls.

Another interesting phenomena that can be ''probed'' using the high sensitivity of the spin-polarized tunnel transport is the reversible character of the AF's net magnetic-moment reversal by coherent rotation. This is illustrated by the R-H minor-loop measurements shown in Fig. 4(b). In this case the external field was stopped in an incomplete AF reversal state after the switching of the DL in negative field, then reduced and finally increased back again. Repeating this process for two points [Fig. 4(b), points (1) and (2)], fully reversible features have been observed. This implies that the magnetization reversal is a fully reversible process that can only be explained through a fully magnetization-rotation mechanism, directly related to the angular distribution of local anisotropies in polycristalline materials.

For preventing all their negative effects on the magnetoresistive response of potential spin-electronics devices, the creation of the 360° walls has to be inhibited. This can be achieved by inducing an anisotropy in an AF system, i.e., by exchange coupling the AF structure with a standard antiferromagnet (IrMn, PtMn) or by growing the magnetic layers in an external field.

V. CONCLUSION

By analyzing the tunnel-magnetoresistive signal shape and amplitude, micromagnetic features in each layer of an artificial ferrimagnet system have been selectively studied. This is made possible by the high sensitivity of the spin polarized current to fluctuations of magnetization in one of the magnetic layers of the magnetic-tunnel junctions. We propose a simple analytical model for the MTJ in a multidomain state, which takes into account different tunneling paths associated to local magnetization configurations. The model allows a quantitative correlation between the spin-polarized transport characteristics and the field-dependent domain structure. The results extracted from the tunnel-magnetoresistance analysis are found to be in good agreement with the data extracted from the analysis of the magnetic-force-microscopy images.

The magnetic state versus field of the magnetic layers constituting the AF was probed selectively in the field window from positive to negative saturation. Hysteretic features were analyzed and attributed to domain-wall creation and annihilation in the AF layers. These effects were interpreted

in the framework of randomly distributed anisotropy axes in polycrystalline films. From our understanding of the magnetic behavior of the AF, it appears that a key parameter to avoid the formation of domain walls during the reversal process would be to induce a uniaxial anisotropy in the hard subsystem to force the magnetization to rotate uniformly. Therefore, to control and optimize the field response of magnetic thin-film devices, hard magnetic AF subsystems are nowadays used with adjacent antiferromagnets or uniaxial anisotropy.

ACKNOWLEDGMENTS

The authors thank illuminating discussions with V. da Costa, Pierre Panissod, H. van den Berg, and Ursula Ebels and experimental support of Yves Henry, Cristian Meny, and Gerard Wurz. This work was supported by the European Framework IV Materials Technology Program, Contract No. BRPR-CT98-0657, the *Dynaspin* program, *Training and Mobility of Researchers* network under Contract. No. FMRX-CT97-0147, and the Nanomem Program (IST-1999-13741). K.O. also acknowledges NSF Grant No. CNRS-9603252.

[1] J.S. Moodera, L.R. Kinder, T.M. Wong, and R. Meservey, Phys. Rev. Lett. **74**, 3273 (1995); T. Miyazaki and N. Tezuka, J. Magn. Magn. Mater. **139**, L231 (1995).

[2] W.J. Gallagher, S.S.P. Parkin, Y. Lu, X.P. Bian, A. Marley, K.P. Roche, R.A. Altman, S.A. Rishton, C. Jahnes, T.M. Shaw, and G. Xiao, J. Appl. Phys. **81**, 3741 (1997).

[3] E. Nowak, R.D. Merithew, M.B. Weissman, I. Bloom, and S.S.P. Parkin, J. Appl. Phys. **84**, 6195 (1998).

[4] S. Gider, B.-U. Runge, A.C. Marley, and S.S.P. Parkin, Science **281**, 797 (1998).

[5] K.S. Moon, R.E. Fontana, S.S.P. Parkin, Appl. Phys. Lett. **74**, 3690 (1999).

[6] C. Tiusan, T. Dimopoulos, K. Ounadjela, M. Hehn, H.A.M. van den Berg, Y. Henry, and V. Da Costa, Phys. Rev. B **61**, 580 (2000).

[7] M. Hehn, O. Lenoble, D. Lacour, C. Fery, M. Piecuch, C. Tiusan, and K. Ounadjela, Phys. Rev. B **61**, 11 643 (2000).

[8] A. Anguelouch, B. Shrang, G. Xiao, Y. Lu, P. Trouilloud, W.J. Gallagher, S.S.P. Parkin, Appl. Phys. Lett. **76**, 622 (2000).

[9] L. Thomas, M.G. Samant, and S.S.P. Parkin, Phys. Rev. Lett. **84**, 1816 (2000).

[10] C. Tiusan, M. Hehn, K. Ounadjela, Y. Henry, J. Hommet, C. Meny, H.A.M. van den Berg, L. Baer, and R. Kinder, J. Appl. Phys. **8**, 5276 (1999).

[11] H.A.M. van den Berg, W. Clemens, G. Gieres, G. Rupp, M. Vieth, J. Wecker, and S. Zoll, J. Magn. Magn. Mater. **165**, 524 (1997).

[12] T. Dimopoulos, C. Tiusan, K. Ounadjela, M. Hehn, and H.A.M. van den Berg, J. Appl. Phys. **87**, 4685 (2000).

[13] N. Persat, H.A.M. van den Berg, K. Cherifi-Khodjaoui, and A. Dinia, J. Appl. Phys. **81**, 4748 (1997); N. Persat, H.A.M. van den Berg, and A. Dinia, J. Magn. Magn. Mater. **165**, 446 (1997).

[14] D.V. Berkov and N.L. Gorn, Phys. Rev. B **57**, 14 332 (1998).

[15] J. Nassar, M. Hehn, A. Vaures, F. Petroff, and A. Fert, Appl. Phys. Lett. **73**, 698 (1988).

[16] E.C. Stoner and E.P. Wohlfarth, Philos. Trans. R. Soc. London, Ser. A **240**, 559 (1948).

[17] R.L. Stamps, A.S. Carrico, and P.E. Wigen, Phys. Rev. B **55**, 6473 (1997).

[18] The polycrystalline Co layers, constituted of small magnetic grains coupled by exchange interactions, are macroscopically magnetically isotropic due to a random orientation of the easy magnetic axis of each grain. For the thickness range and weak intergrain coupling involved in our samples, the reversal of the layer magnetization proceeds mainly by individual grain magnetic-moment rotation (Ref. 14). During the magnetization reversal, moments inside areas presenting the smallest coupling (direct lateral-exchange coupling and/or indirect AF interlayer coupling) start to rotate, and drag in rotation the magnetization inside neighbor areas with stronger coupling. The sense of rotation is determined by a local effective anisotropy. Therefore, separate domains with rotating magnetization turn clockwise or counterclockwise leading to the appearence of 360° Néel domain walls.

[19] C. Tiusan, M. Hehn, T. Dimopoulos, and K. Ounadjela, J. Appl. Phys. **89**, 6668 (2001).